

Journal of Materials Chemistry A

Accepted Manuscript



This is an *Accepted Manuscript*, which has been through the Royal Society of Chemistry peer review process and has been accepted for publication.

Accepted Manuscripts are published online shortly after acceptance, before technical editing, formatting and proof reading. Using this free service, authors can make their results available to the community, in citable form, before we publish the edited article. We will replace this *Accepted Manuscript* with the edited and formatted *Advance Article* as soon as it is available.

You can find more information about *Accepted Manuscripts* in the [Information for Authors](#).

Please note that technical editing may introduce minor changes to the text and/or graphics, which may alter content. The journal's standard [Terms & Conditions](#) and the [Ethical guidelines](#) still apply. In no event shall the Royal Society of Chemistry be held responsible for any errors or omissions in this *Accepted Manuscript* or any consequences arising from the use of any information it contains.

Cite this: DOI: 10.1039/c0xx00000x

ARTICLE TYPE

www.rsc.org/xxxxxx

Enhanced cycle performance of Li-S battery based on protected lithium anode

Guoqiang Ma^a, Zhaoyin Wen^{*a}, Qingsong Wang^a, Chen Shen^a, Jun Jin^a, Xiangwei Wu^a⁵ Received (in XXX, XXX) Xth XXXXXXXXX 20XX, Accepted Xth XXXXXXXXX 20XX

DOI: 10.1039/b000000x

A conductive polymer layer is prepared on the surface of lithium anode as the protective layer for Li-S battery. With the protective layer, a stable and less resistive SEI is formed between the ether-based electrolyte and Li anode, it can not only inhibit the corrosion reaction between lithium anode and lithium polysulfides effectively, but also suppress the growth of Li dendrites. Particularly, with approximately 2.5-3 mg.cm⁻² sulfur loading on the electrode and commercial electrolyte, the discharge capacity retains at 815mAh.g⁻¹ after 300 cycles at 0.5C with an average coulombic efficiency of 91.3%.

Introduction

Currently, with the rapid development of advanced portable devices, zero-emission electric vehicles (EV) and smart grids, rechargeable batteries with high energy density and long cycle life are in given great demand¹. Among various battery systems, sulfur cathode has a high theoretical capacity (1675mAh.g⁻¹) and a high theoretical specific energy (2600Wh.Kg⁻¹)². In combination with the natural abundance, low cost and environmental friendliness of sulfur, the Li-S battery becomes a promising candidate for the next generation^{3,4}.

However, the insulating nature of sulfur, the volume expansion, and the high solubility of lithium polysulfides (PS) in the ether-based electrolyte lead to a high polarization, serious capacity fading, poor rate stability and low coulombic efficiency of Li-S battery, inhibiting its commercialization. Many approaches have been made to address these obstacles and improve the electrochemical performance of Li-S battery⁵⁻⁸. Most studies are focusing on the modification of cathode with various kinds of carbon materials and conductive polymers⁹⁻¹¹. All the approaches can enhance the electrical conductivity of the cathode and suppress the loss of soluble polysulfides intermediates during cycling, and thereby improve the active material utilization and cyclability. In addition, the issue of low coulombic efficiency has been improved by the addition of lithium nitrate in the electrolyte¹². However, there are few reports on the improvement of lithium anode for Li-S battery, whose problems are complex and severe, and it could be a new strategy for improving the performance of the Li-S battery³.

Li anode for Li-S battery suffers from several problems. Firstly, lithium is so reactive that the electrolyte can be reduced to form a solid electrolyte interphase (SEI) layer, causing a remarkable

irreversible capacity loss and low deposition efficiency of Li upon charging^{3,13}. For practical Li-S batteries, this condition may lower the energy output of the system by requiring an excessive amount of Li to pair with S cathode. Secondly, the growth of Li dendrites originating from an uneven deposition of Li can cause safety problems. Although, the dendrite issue is unique for the Li-S battery because of the soluble polysulfides, which possibly suppress the growth of Li dendrite^{13,14}. The third problem of the Li anode arises from the undesired shuttle effect of lithium polysulfides. Soluble lithium polysulfides diffusing throughout the separator could react with Li anode to form the insoluble and insulating sulfides (Li₂S₂, Li₂S) on the surface of lithium anode¹⁵. The insulating lithium sulfides can retard the rapid transportation of Li, resulting in poor rate capability, lack of totally reversibility during the following cycles¹⁶. The solid polymer electrolyte¹⁷ with Li⁺ conductivity and sulfur power¹⁸ have been employed to protect Li anode during charge/discharge process. However, more effective and simple approaches are necessary to solve the problems of Li anode.

Coating layer with conductive polymers, such as poly(3,4-ethylenedioxythiophene)¹⁹ (PEDOT), polypyrrole (PPy)^{20,21}, and polyaniline (PANI)^{22,23} on sulfur cathode has been proved to improve the performance. Recently, Cui's group found that the capability of PEDOT in improving long-term cycling stability and high-rate performance of the sulfur cathode is the best among the three polymers¹¹. It is thus interesting to further investigate a PEDOT-based ion conductive copolymer as a protection layer on the surface of the lithium metal. Among the PEDOT-based copolymers, poly(3,4-ethylenedioxythiophene)-co-poly(ethylene glycol) (PEDOT-co-PEG) is a promising candidate. Firstly, the PEDOT-co-PEG copolymer possesses strong adhesive properties to a lithium surface, which makes it effective for mechanically suppressing Li-dendrite growth²⁴. Additionally, PEG is a highly

ion-conductive polymer that transports lithium ions, which is usually introduced into sulfur composites to inhibit the diffusion of polysulfides out of the cathode and relieve the volumetric expansion of sulfur²⁵.

Herein, as shown in Fig. 1, PEDOT-co-PEG is coated onto lithium anode using a simple and low cost method as a functional protective layer. The thin protection layer with strong adhesion to the lithium electrode is beneficial to form a stable and less resistive SEI between the anode and electrolyte. Moreover, it can restrict the access of the lithium polysulfides to the Li anode physically, suppressing the undesired corrosion reaction. Therefore, it is predictable for the Li-S battery with protected lithium anode to give an excellent electrochemical performance.

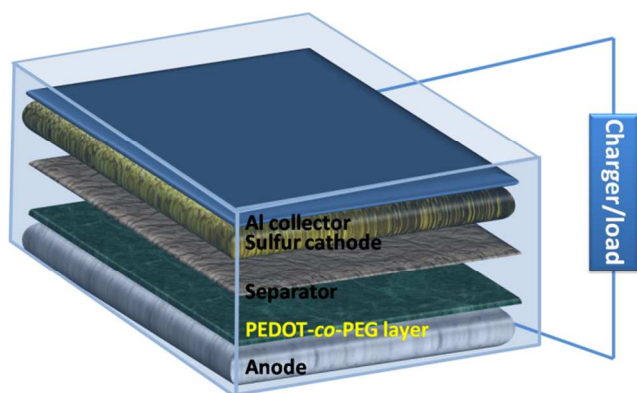


Fig. 1. Scheme of Li-S battery with PEDOT-co-PEG protected lithium sheet as the anode.

Experimental

The protection of the lithium anode

The PEDOT-co-PEG solution (1 wt% dispersion in nitromethane) was purchased from Sigma Aldrich and used as received. The lithium metal with PEDOT-co-PEG protective layer is prepared as follows: Lithium metal was directly immersed into the polymer solution in a dry box filled with argon gas. After 12h, the polymer-coated lithium electrode was rinsed with dimethyl ether(DME) and dried for 24 h. To obtain a sufficiently thick protective layer on the surface of lithium metal, the process mentioned above was repeated for 4-5 times. The thickness of the protective layer was around 10 μ m.

Preparation of sulfur cathode

The S/C composite was prepared by a melting diffusion strategy with a mixture of sulfur and Ketjen black (KB) (Akzo Nobel Corp.) in the weight ratio of 2:1, respectively. Then the composite was sealed in a glass tube under vacuum followed by co-heating at 155 °C for 12 h. Consequently, the slurry was prepared by ball milling 80% S/C composite, 10wt% acetylene black (AB) as conductive agent, 5wt% carboxy methyl cellulose (CMC), 5wt% (styrene-butadiene rubber) SBR as binders and deionized water as the solvent. The slurries were casted onto aluminum foil substrates. After the solvent was evaporated, the electrode was cut into discs with 14 mm in diameter and then dried at 60 °C under vacuum for 12 h. Accordingly, the sulfur loading in the cathode was around 2.5-3 mg.cm⁻². CR2025 type

coin cells were assembled in a glove box with oxygen and water contents less than 1 ppm. The electrolyte consisted of 1M LiN(CF₃SO₂)₂ (LiTFSI) in a mixed solvent of 1,3-dioxolane (DOL) and dimethyl ether(DME). The cells contained Celgard 2400 as the separator and lithium foils as both the counter and reference electrodes. The Li/electrolyte/Li cells are prepared with symmetrical lithium metal as the anode and cathode.

Characterization

SEM images were measured by field emission scanning electron microscope (FESEM JSM-6700) and scanning electron microscope (Hitachi S-3400N). AC impedance measurement was carried out by a Frequency Response Analyzer (FRA) technique on an Autolab Electrochemical Workstation over the frequency range from 0.1 Hz to 10 MHz with the amplitude of 10 mV. The galvanostatic charge and discharge tests were conducted on a LAND CT2001A battery test system in a voltage range of 1.8-2.6 V (vs. Li/Li⁺) at 0.2C and 0.5C (1C=1675mA.g⁻¹).

Results and discussion

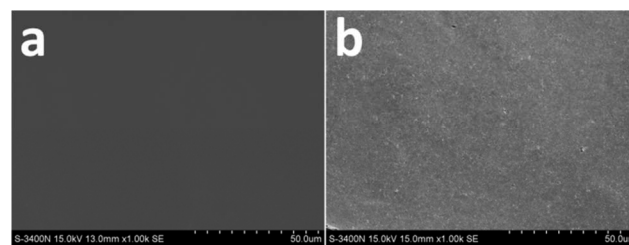


Fig. 2. SEM images of the surfaces of the (a) pristine lithium electrode and (b) surface-modified lithium electrode with PEDOT-co-PEG copolymer.

Fig. 2a and Fig. 2b show the morphology of a lithium sheet before and after surface coating with PEDOT-co-PEG. As shown, the surface of the pristine lithium sheet is smooth while the one with PEDOT-co-PEG coating has a rough surface. Indicating that the polymer is fully covered on the surface of the lithium electrode.

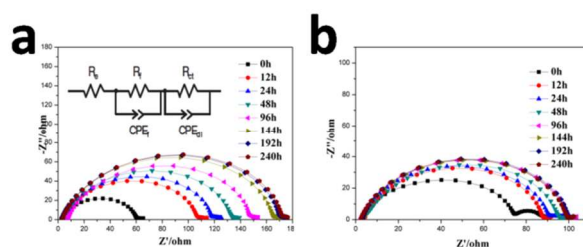


Fig. 3. AC impedance spectra of the Li/electrolyte/Li cells with (a) pristine and (b) surface protected Li electrodes as a function of storage time at 25°C.

The lithium sheet with PEDOT-co-PEG as the protective layer is beneficial to form a stable and less resistive SEI in the carbonate-based electrolyte²⁴. To investigate the interfacial stability of the protected lithium anode in the ether-based electrolyte, AC impedance measurements of Li/electrolyte/Li cells are performed²⁶. As seen in Fig. 3a and Fig. 3b, the spectra are composed of two partially overlapping semicircles at high and low frequency regions respectively. The semicircle at high

frequency corresponds to the SEI, and the low frequency semicircle is related to the charge transfer process between the electrode and electrolyte.

These spectra could be analyzed using the equivalent circuit given in the inset of the Fig.3a. In this circuit, R_e is the electrolyte resistance, which corresponds to the high frequency intercept at the real axis. R_f and R_{ct} are the resistance of the SEI film and the charge transfer resistance, respectively. In the cell assembled with the pristine Li electrode, the initial resistances of the cell (R_f and R_{ct}) are less than those of the cell using a PEDOT-co-PEG protecting Li electrode, indicating the existing of protective layer on the surface of lithium anode^{24, 26}. However, the R_f value increases from 59Ω to 172Ω after 192h, owing to the gradual growth of SEI between the lithium electrode and the electrolyte. In the cell assembled with the surface-modified Li electrode, R_f initially increases to the maximum value after 96h and stabilizes at around 99Ω , indicating the suppression of deleterious reactions between the PEDOT-co-PEG protecting lithium electrode and the ether-based electrolyte solution. As a result, the interfacial stability of the lithium electrode is improved because of the a protective layer.

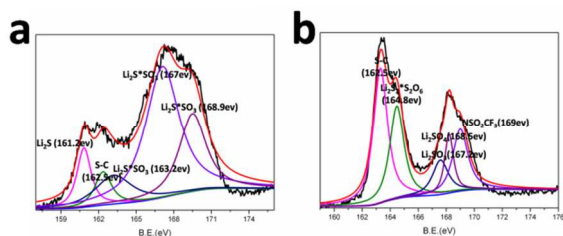


Fig. 4 XPS spectra (S peak) of Pristine Li (a) and PEDOT-co-PEG protected Li (b) surfaces stored for 8 days in the electrolyte.

To understand the chemical state of the surface film on the lithium electrode after stored in the electrolyte, chemical composition and depth profile information of the surface film were obtained by X-ray photoelectron microscopy spectra (XPS). As shown in Fig.4, S-C, Li_2S , Li_2S*SO_3 are all the products of the between Li and TFSI anion and electrolyte solvent reduction, while the insulating Li_2S can't be observed in that of PEDOT-co-PEG protected Li anode²⁷. And more stable Li_2SO_x (Li_2SO_3 , Li_2SO_4 and $Li_2S_2*S_2O_6$) is found in the PEDOT-co-PEG protected Li anode, they have been found in the Li anode for Li-S battery in the electrolyte with $LiNO_3$, showing that a more stable SEI is formed between PEDOT-co-PEG protecting Li anode and the electrolyte^{27, 28}.

The initial charge/discharge profiles at different cycles of Li-S batteries assembled with different lithium electrodes are shown in Fig.5a, there are two discharge plateaus at 2.3V and 2.1V, corresponding to the generation of lithium polysulfides and Li_2S/Li_2S_2 ^{25, 29}. And charge/discharge profiles are similar, indicating that the protective layer on the surface of lithium anode doesn't change the electrochemical reactions. For coin battery, lithium anode is far from sufficient with respect to the active material in the sulfur cathode, so the initial discharge capacity is determined by the state of sulfur cathode. Therefore, Li-S battery with pristine Li electrode shows a close initial discharge capacity compared to that of Li-S battery with PEDOT-co-PEG protected lithium anode.

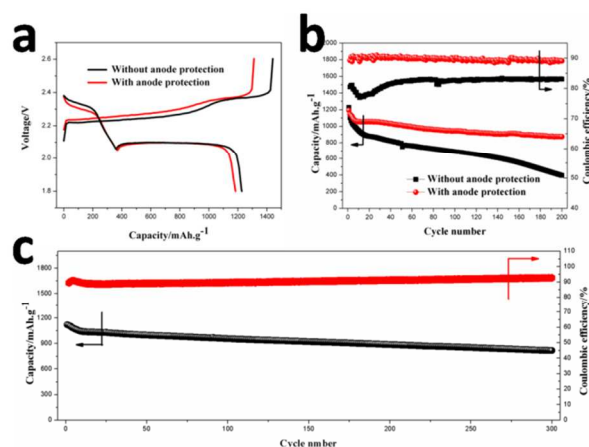


Fig. 5 (a) The charge/discharge profiles at different cycles of Li-S battery assembled with protected Li anode. (b) The cycle performance of Li-S batteries assembled with different Li anodes at 0.2C. (c) The cycle performance of Li-S batteries assembled with protective Li anodes at 0.5C.

The cycle performance and coulombic efficiency of Li-S batteries assembled with different lithium electrodes are shown in Fig. 5b. The called "shuttle effect" is one of the most important reasons for the poor cycle performance and low coulombic efficiency of Li-S battery⁵. However, as mentioned above, once lithium anode is protected by PEDOT-co-PEG layer, the contact between lithium anode and lithium polysulfides is restricted, so the corrosion reaction between them during the discharge process is suppressed effectively. Furthermore, more insulating Li_2S/Li_2S_2 aggregated on the surface of the conductive PEDOT-co-PEG layer will be transformed to the soluble Li_2S_x during the charge process. Consequently, the low coulombic efficiencies, redistribution of active material and rapid capacity fading of the common Li-S battery are suppressed significantly. As shown, the discharge capacity of Li-S battery with protected Li anode maintains a high capacity of $875.6\text{mAh}\cdot\text{g}^{-1}$ at 0.2C with a good capacity retention of 73.45% after 200cycles, while Li-S battery with pristine Li anode shows a capacity of $399.8\text{mAh}\cdot\text{g}^{-1}$ at 0.2C with a poor capacity retention of 32.8%. Moreover, the average coulombic efficiency of Li-S battery with protected Li anode is as high as 89.2% in the electrolyte without $LiNO_3$, which is much higher than that of 80.7% for Li-S battery with pristine Li anode. The Li-S battery with the protected Li anode also shows excellent cycle performance at 0.5C, the specific capacity retains at $815\text{mAh}\cdot\text{g}^{-1}$ even after 300 cycles with the average coulombic efficiency of 91.3%.

Although the addition of $LiNO_3$ in the electrolyte can increase the coulombic efficiency of Li-S battery, it was reported that the electrolyte with $LiNO_3$ added can oxidize sulfur compounds to higher and irreversible oxidation states, such as Li_xSO_y species³⁰. Moreover, the decomposition of $LiNO_3$ will generate gas during charge/discharge. The Li-S battery with PEDOT-co-PEG protected Li anode shows excellent cycle stability and improved coulombic efficiency in the electrolyte without $LiNO_3$, which can avoid the disadvantages of $LiNO_3$ additives.

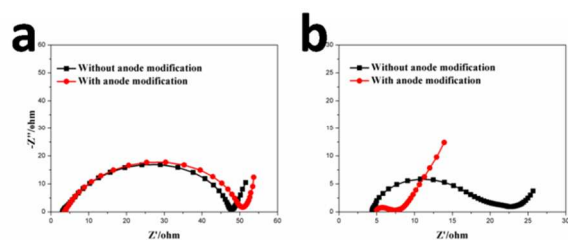


Fig. 6 AC impedance spectra before (a) and after 100 cycles (b) of Li-S batteries assembled with different lithium anode.

Furthermore, the electrochemical behavior of Li-S batteries assembled with different lithium anodes before and after 100 cycles is investigated by electrochemical impedance spectroscopy (EIS). As shown in Fig. 6, there is a compressed semicircle at the high frequency corresponding to the charge transfer resistance and SEI layer and a sloped straight line in the low frequency domain corresponding to the Warburg impedance^{31, 32}. The impedance value of the batteries with and without proactive Li anode are very close before cycling, showing the conductive polymer coating layer doesn't change the fast ion transport behavior of lithium anode. The redistribution of the insulating sulfur besides cathode (on the surface of the cathode, the separator and the anode) during charge/discharge process is the main reason for the increased resistance^{16, 32}. As shown, after 100 cycles, the Li-S battery with protected Li anode revealed a much smaller interfacial resistance than the cell with the pristine Li electrode, implying the cell with the modified Li electrode has a more stable and less resistive SEI layer that facilitated more efficient lithium ion transfer at the interfaces during cycling. And the redistribution of insulating active material during charge/discharge process are suppressed effectively, indicating a suppressed shuttle effect.

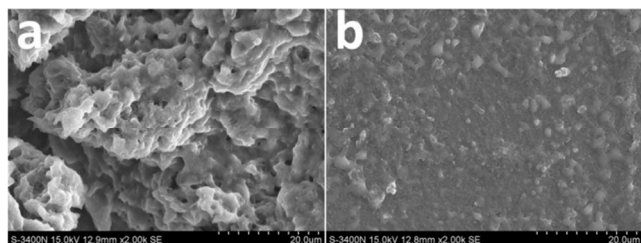


Fig. 7 The surface morphologies of the Li anode after 100 cycles: (a) the pristine Li anode; (b) the surface-protected Li anode.

Fig. 7 comparatively shows the surface morphology of the Li anode with and without protective layer after 100 cycles. The Li anode is disassembled from the cycled cell carefully before the SEM images are acquired. The surface of pristine lithium anode after 100 cycles is loosely packed, suggesting serious dendrite growth and corrosion reaction. The protected Li anode showed a relatively smoother and denser surface morphology than the non-protected one. These results suggest that the PEDOT-*co*-PEG protection layer on the lithium electrode can suppress the corrosion reaction and dendrite growth effectively.

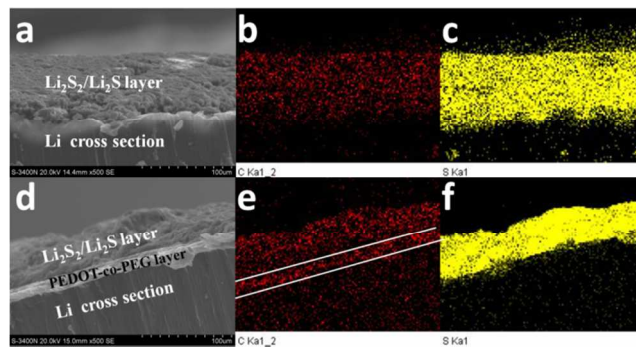


Fig. 8 The cross section morphology(a, d) and EDS mapping element of carbon(b, e) and sulfur (c, f) of pristine Li anode and protected Li anode after 100 cycles.

As for Li-S battery with pristine Li anode, the corrosion reaction between lithium polysulfides and Li anode results in continuous loss of active material and an increased thickness $\text{Li}_2\text{S}_2/\text{Li}_2\text{S}$ layer on the surface of metal anode. As seen in Fig. 8a, Fig. 8b and Fig. 8c, the thickness of $\text{Li}_2\text{S}_2/\text{Li}_2\text{S}$ layer on the surface of pristine lithium anode is as high as $100\mu\text{m}$, and the contact place between Li cross section and $\text{Li}_2\text{S}_2/\text{Li}_2\text{S}$ layer is uneven, indicating a serious corrosion reaction during charge/discharge process¹⁶. However, as seen in Fig. 8d, Fig. 8e and Fig. 8f, the thickness of $\text{Li}_2\text{S}_2/\text{Li}_2\text{S}$ layer is only about $40\mu\text{m}$, which is much thinner than that of pristine lithium anode. The thickness of PEDOT-*co*-PEG protecting layer is around $10\mu\text{m}$. The contact areas between the PEDOT-*co*-PEG and the $\text{Li}_2\text{S}_2/\text{Li}_2\text{S}$ layer are both self-evident relatively. And it remains undamaged even after prolonged cycles, indicating a strong adhesive and excellent mechanical properties to a lithium surface and a good mechanically suppression to the Li-dendrite growth. Moreover, the undesired corrosion reaction is suppressed effectively when the lithium anode is protected with PEDOT-*co*-PEG polymer.

Conclusions

Lithium anode is protected with PEDOT-*co*-PEG polymer using a simple, novel and low cost method. Firstly, the thin PEDOT-*co*-PEG layer formed on the surface of lithium metal stabilizes the interface of lithium anode in the prolonged contact with the ether-based electrolyte. Secondly, the contact between lithium anode and lithium polysulfides is obstructed physically, suppressing the undesired corrosion reaction. Thirdly, the protective layer shows a strong adhesive properties to a lithium surface and good mechanical, suppressing the Li-dendrite growth during charge/discharge process. Therefore, with the addition of protective layer, a stable and less resistive SEI is formed, the shuttle effect and dendrite growth on the surface of lithium anode is suppressed effectively, resulting in an excellent cycling stability and a high coulombic efficiency.

Acknowledgements

This work was financially supported by NSFC Project No.51373195, No.51201177 and No. 51272267; research projects from the Science and Technology Commission of Shanghai Municipality No. 08DZ2210900.

Notes and references

- ^a CAS Key Laboratory of Materials for Energy Conversion, Shanghai Institute of Ceramics, Chinese Academy of Sciences, Shanghai, China, 200050
Tel: +86-21-52411704; Fax: +86-21-52413903;
E-mail: zywen@mail.sic.ac.cn
1. S. A. F. Peter G. Bruce, Laurence J. Hardwick and Jean-Marie Tarascon, *Nat Mater.* 2012, **11**(1), 19.
 2. A. Manthiram, Y. Fu, S.-H. Chung, C. Zu and Y.-S. Su, *Chem Rev.* 2014, 140715153614001.
 - 10 3. Y. X. Yin, S. Xin, Y. G. Guo, L. J. Wan, *Angewandte Chemie International Edition.* 2013, **52**(50), 13186.
 4. Y. Yang, G. Zheng and Y. Cui, *Chem Soc Rev.* 2013, **42**, 3018.
 5. D.-W. Wang, Q. Zeng, G. Zhou, L. Yin, F. Li, H.-M. Cheng, I. R. Gentle and G. Q. M. Lu, *Journal of Materials Chemistry A*, 2013, **1**, 9382.
 - 15 6. S. S. Zhang, *J Power Sources*, 2013, **231**, 153-162.
 7. H. Kim, H.-D. Lim, J. Kim and K. Kang, *Journal of Materials Chemistry A*, 2014, **2**, 33.
 8. J. W. Kim, J. D. Ocon, D. W. Park, J. Lee. *ChemSusChem.* 2014, 20 7(5), 1265
 9. G. Zhou, S. Pei, L. Li, D.-W. Wang, S. Wang, K. Huang, L.-C. Yin, F. Li and H.-M. Cheng, *Adv Mater.* 2014, **26**, 625-631.
 10. G. He, S. Evers, X. Liang, M. Cuisinier, A. Garsuch and L. F. Nazar, *Acs Nano*, 2013, **7**, 10920-10930.
 - 25 11. W. Li, Q. Zhang, G. Zheng, Z. W. Seh, H. Yao and Y. Cui, *Nano Lett.* 2013, **13**, 5534-5540.
 12. X. Liang, Z. Y. Wen, Y. Liu, M. F. Wu, J. Jin, H. Zhang, X. W. Wu, *J Power Sources.* 2011, **196**, 9839.
 13. D. Aurbach, E. Pollak, R. Elazari, G. Salitra, C. S. Kelley and J. 30 Affinito, *Journal of the Electrochemical Society*, 2009, **156**, A694-A702.
 14. Y. Mikhaylik, I. Kovalev, R. Schock, K. Kumaresan, J. Xu and J. Affinito, *Battery/Energy Technology (General) - 216th Ecs Meeting*, 2010, **25**, 23-34.
 - 35 15. X. Ji and L. F. Nazar, *J Mater Chem*, 2010, **20**, 9821.
 16. J. Zheng, M. Gu, C. Wang, P. Zuo, P. K. Koech, J. G. Zhang, J. Liu and J. Xiao, *Journal of the Electrochemical Society*, 2013, **160**, A1992-A1996.
 17. Y. M. Lee, N.-S. Choi, J. H. Park and J.-K. Park, *J Power Sources*, 40 2003, **119-121**, 964-972.
 18. R. Demir-Cakan, M. Morcrette, Gangulibabu, A. Guéguen, R. Dedryvère and J.-M. Tarascon, *Energ Environ Sci*, 2013, **6**, 176.
 19. H. Chen, W. Dong, J. Ge, C. Wang, X. Wu, W. Lu and L. Chen, *Sci Rep.*, 2013, **3**, 01910-01915.
 - 45 20. C. Wang, W. Wan, J.-T. Chen, H.-H. Zhou, X.-X. Zhang, L.-X. Yuan and Y.-H. Huang, *Journal of Materials Chemistry A*, 2013, **1**, 1716.
 21. J. Shao, X. Li, L. Zhang, Q. Qu and H. Zheng, *Nanoscale*, 2013, **5**, 1460.
 22. W. Zhou, Y. Yu, H. Chen, F. J. DiSalvo and H. D. Abruña, *J Am Chem Soc*, 2013, **135**, 16736-16743.
 - 50 23. L. Xiao, Y. Cao, J. Xiao, B. Schwenzer, M. H. Engelhard, L. V. Saraf, Z. Nie, G. J. Exarhos and J. Liu, *Adv Mater.* 2012, **24**, 1176-1181.
 24. I. S. Kang, Y. S. Lee and D. W. Kim, *Journal of the Electrochemical Society*, 2013, **161**, A53-A57.
 - 55 25. L.-X. Miao, W.-K. Wang, A.-B. Wang, K.-G. Yuan and Y.-S. Yang, *Journal of Materials Chemistry A*, 2013, **1**(38), 11659-11664.
 26. M. Wu, Z. Wen, Y. Liu, X. Wang and L. Huang, *J Power Sources*, 2011, **196**, 8091-8097.
 - 60 27. Aurbach D, Pollak E, Elazari R, et al. *Journal of the Electrochemical Society*, 2009, **156**(8), A694-A702.
 28. S. Xiong, K. Xie, Y. Diao and X. Hong, *J. Power Sources*, 2013, **236**, 181-187.
 29. C. Zu, Y.-S. Su, Y. Fu and A. Manthiram, *Phys Chem Chem Phys*, 65 2013, **15**, 2291.
 30. Y. Diao, K. Xie, S. Xiong, X. Hong, *Journal of the Electrochemical Society*, 159 (2012) A1816-A1821.
 31. Z. Deng, Z. Zhang, Y. Lai, J. Liu, J. Li and Y. Liu, *Journal of the Electrochemical Society*, 2013, **160**, A553-A558.
 - 70 32. N. A. Cañas, K. Hirose, B. Pascucci, N. Wagner, K. A. Friedrich and R. Hiesgen, *Electrochim Acta*, 2013, **97**, 42-51.
 33. G. Ma, Z. Wen, J. Jin, Y. Lu, K. Rui, X. Wu, M. Wu and J. Zhang, *J Power Sources*, 2014, **254**, 353-359.